PHILOSOPHICAL TRANSACTIONS OF THE ROYAL SOCIETY A MATHEMATICAL, PHYSICAL & ENGINEERING SCIENCES

Intermolecular Interactions and the Nature of Orientational Ordering in the Solid Fullerenes C $_{60}$ and C$_{70}$ [and Discussion]

Ailan Cheng, Michael Klein, Michele Parrinello, Michiel Sprik and M. Lal

Phil. Trans. R. Soc. Lond. A 1992 **341**, 327-336
doi: 10.1098/rsta.1992.0105

Intermolecular interactions and the nature of orientational ordering in the solid fullerenes C_{60} and C_{70}

By Ailan Cheng[1], Michael Klein[1], Michele Parrinello[2] and Michiel Sprik[2]

[1] *Department of Chemistry and Laboratory for Research on the Structure of Matter, University of Pennsylvania, Philadelphia, Pennsylvania 19104–6323, U.S.A.*
[2] *IBM Research Division, Zurich Research Laboratory, 3303 Rüschlikon, Switzerland*

We have proposed an intermolecular potential for C_{60} molecules that not only reproduces the correct low-temperature structure, but also correlates a wide range of experimental properties, including the molecular reorientational time in the room-temperature rotator phase, the volume change at the orientational ordering transition, and the librational frequencies in the low-temperature phase. The low-pressure phases in solid C_{70} have been explored using constant-pressure molecular dynamics and an intermolecular potential derived from one that gives an excellent account of the properties of solid C_{60}. The molecular dynamics calculations predict three low-pressure phases: a high-temperature rotator phase, a partly ordered phase with trigonal symmetry, and an ordered monoclinic phase. The calculations on C_{70} were carried out on a cluster of IBM RS/6000s, operating in parallel.

1. Introduction

Our understanding of solid fullerenes is largely derived from detailed experimental studies on Buckminsterfullerenes (Taylor *et al.* 1990; David *et al.* 1991; Heiney *et al.* 1991; Johnson *et al.* 1991; Neumann *et al.* 1991; Sachidanandum & Harris 1991; Tycko *et al.* 1991*a*, *b*; Yannoni *et al.* 1991; Copley *et al.* 1992; David *et al.* 1992; Heiney *et al.* 1992; van Loosdrecht *et al.* 1992; Shi *et al.* 1992). This new allotrope of carbon, composed of C_{60} clusters, behaves as a typical molecular crystal. The room-temperature structure is a face-centred cubic (FCC) rotator phase, which transforms to an orientationally ordered state at 250 K. The low-temperature structure is simple cubic, with space group $Pa\bar{3}$ (David *et al.* 1991). The observed $Pa\bar{3}$ structure has electron-rich short hexagon bonds facing electron-poor pentagon centres of adjacent molecules. Static structure optimization and molecular dynamics calculations based on atom–atom potentials (Guo *et al.* 1991) have failed to explain the experimental low-temperature $Pa\bar{3}$ structure. Instead, they predict a tetragonal, rather than cubic, low-temperature phase. The discrepancy in the ordered phase is in contrast to the surprisingly accurate description provided by the atom–atom potential of the structure and dynamics of the disordered high-temperature phase (Cheng & Klein 1991). Solid C_{70} has received less attention. Because of the elongated 'rugby ball' shape (Fowler *et al.* 1991; Andreoni *et al.* 1992), the phase diagram of C_{70} will likely be more complex. Indeed, X-ray diffraction measurements (Vaughan *et al.* 1992)

Phil. Trans. R. Soc. Lond. A (1992) **341**, 327–336
Printed in Great Britain

indicate a FCC high-temperature phase, plus phase transitions at about 340 K and 280 K. Neither the molecular ordering nor the lattice symmetry of the low-temperature phases have yet been resolved.

In this paper, we review previous attempts to construct an empirical intermolecular potential for C_{60} molecules. Potentials now exist that not only reproduce the correct low-temperature structure of C_{60}, but also correlate a range of experimental data, including the molecular reorientational time in the room-temperature rotator phase (Johnson *et al.* 1991; Tycko *et al.* 1991), the volume change at the orientational ordering transition (Heiney *et al.* 1992), and the librational frequencies in the low-temperature phase (Copley *et al.* 1992). The potential model has been extended to treat C_{70} and the nature of the low-pressure phases of the solid have been explored using constant-pressure molecular dynamics (MD) calculations (Nosé & Klein 1983; Parrinello & Rahman 1980). The number of interaction sites on a C_{70} molecule is *ca.* 100, so that each pair potential requires evaluation of 100×100 terms. This type of intensive MD calculation is eminently suited to parallel processing. The results of the simulations, carried out on a cluster of IBM RS/6000 workstations, yield predictions concerning the structure of solid C_{70} in its room-temperature phase and the ground state.

2. An intermolecular potential for solid C_{60}

To achieve the level of accuracy mentioned above for C_{60}, it was necessary to explicitly include interaction sites on the electron-rich short C–C bonds, plus an electrostatic contribution to the intermolecular potential. The distinction between the two bond types can be justified qualitatively by experimental (David *et al.* 1991) and theoretical evidence (Fowler *et al.* 1990, 1991) indicating that the conjugation of the π bond network is incomplete; the length of a bond shared by two hexagons is shorter than bonds of the pentagons. The explicit representation of multiple bonds in the modelling of intermolecular interactions has an important precedent in the study of solid nitrogen, where it proved necessary to place a third interaction centre in the middle of the triple bond (Raich & Mills 1971).

The situation for C_{60} at low pressure is akin to high-pressure nitrogen, because carbon atoms at the sites where the C_{60} molecules make contact are pressed together by the large cohesive forces of all the other atoms. Thus, local C–C contacts in solid C_{60} are actually much closer than those between lamella in graphite. In C_{60}, contacts are optimized when a short C–C bond is wedged into the centre of a pentagon and the distance between bonds maximized (David *et al.* 1991). On the other hand, the spurious tetragonal structure favoured by the atom–atom potential model is characterized by crossed short bonds at minimum separation (Guo *et al.* 1991; Cheng & Klein 1992*a*).

In the interacting bond model of Sprik *et al.* (1992), the 60 Lennard–Jones carbon sites of C_{60} were supplemented with 30 sites D, located at the centres of the double bonds. The molecule was treated as a rigid framework of atoms and bonds, with the geometry taken from Fowler *et al.* (1991) and Feuston *et al.* (1991). In addition, the modelling of solid nitrogen suggested a way to further refine the potential. The nitrogen molecule, as a consequence of the triple bond, carries an appreciable electrostatic quadrupole moment. The corresponding intermolecular coupling in C_{60}, which involves $l = 6, 10, 18, \ldots$ spherical harmonics, cannot be ignored in a description of the solid (Michel *et al.* 1992). To account for this important electrostatic component, Sprik *et al.* (1992) assigned a negative bond charge q_D to

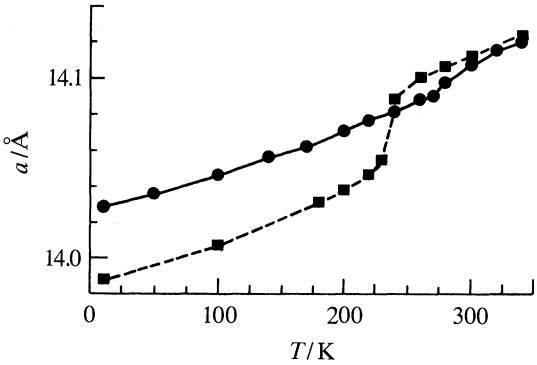

Figure 1. The squares and dots indicate the calculated temperature dependence of the cubic lattice parameters of solid C_{60} for the models of Sprik *et al.* (1992*a*, *b*) and Lu *et al.* (1992) respectively.

the D sites, and a compensating positive charge $q_C = -\frac{1}{2}q_D$ to the C atoms. As a result, the pentagons acquired a total charge of $5q_C$. The D sites are attracted by this net accumulation of positive charge, which, in turn, enhances the stability of the observed $Pa\bar{3}$ structure. In this formulation of the intermolecular potential, the electrostatic contribution to the orientational ordering is important but secondary to the short-range repulsion on the D sites. The potential parameters $\sigma_{CD} = 3.4$ Å†, and $\sigma_{DD} = 3.6$ Å were fixed and ϵ and q_D adjusted to yield reasonable values for the transition temperature (Dworkin *et al.* 1991), the cohesive energy (Pan *et al.* 1991), the reorientational relaxation time in the disordered phase (Johnson *et al.* 1991; Tycko *et al.* 1991*a*, *b*), plus the librational spectrum in the ordered phase (Copley *et al.* 1992). With a value of $q_D = -0.35e$ and $\epsilon = 15$ K, there is reasonable overall agreement among all four properties.

The calculations required for the parameter fitting were performed using a constant pressure-constant temperature molecular dynamics algorithm (Nosé & Klein 1983; Parrinello & Rahman 1980), and systems of 32 or 108 molecules, replicated by periodic boundary conditions (Allen & Tildesley 1987). The length of a run at a single state point was typically between 50 and 100 ps. The calculated structural transformation is an abrupt event (see figure 1) occurring around 225 K, which is somewhat lower than the experimental value of *ca.* 250 K. The transformation is clearly first order, with a modest hysteresis (Sprik *et al.* 1992). The calculated discontinuity agrees well with recent measurements (Heiney *et al.* 1992). The total binding energy of the model compares favourably with the measured enthalpy of formation $\Delta H = 171$ kJ mol^{-1} (Pan *et al.* 1991). Figure 2 contains snapshots of typical configurations from the high and low-temperature phases of C_{60}.

The effect of pressure on the orientational transition temperature T_t was also investigated with the result $(dT_t/dP) = 12 \pm 4$ K kbar^{-1}‡, which is in reasonable accord with the experimental coefficient 11.7 K bar^{-1} (Kriza *et al.* 1991). The spectral density of the librational modes in the ordered phase at 100 K was calculated. The band of librational frequency was recently measured experimentally to be centred around 20 cm^{-1} (Copley *et al.* 1992), in fair agreement with the present model, which yields 15 cm^{-1}. The relaxation time of orientational correlations in the disordered phase obtained from NMR studies at 300 K was determined by Tycko *et al.* (1991*a*, *b*) and Johnson *et al.* (1992) as 12 ps and 8 ps respectively. The result from the MD calculations was 9 ± 2 ps.

† Å $= 10^{-10}$ m $= 10^{-1}$ nm. ‡ 1 bar $= 10^5$ Pa.

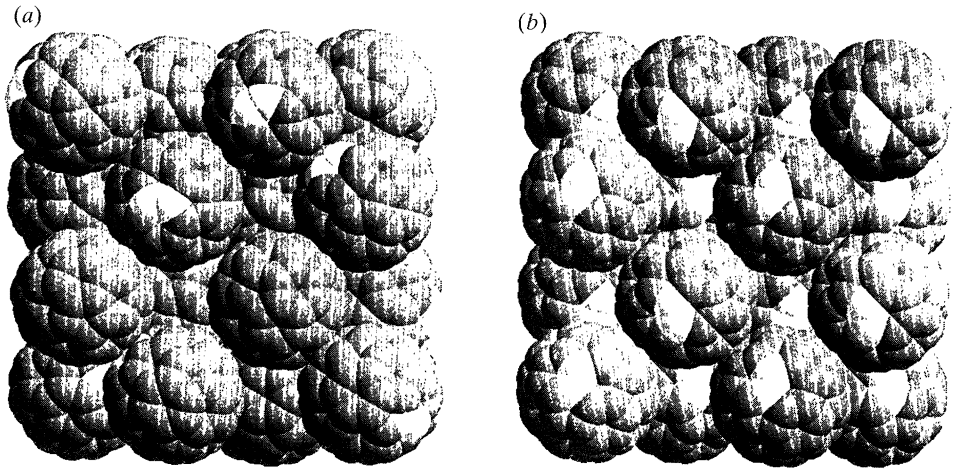

Figure 2. Instantaneous configurations taken from molecular dynamics simulations of the fullerene C_{60}. (*a*) The room-temperature rotator phase. (*b*) The low-temperature ordered phase.

The performance of the intermolecular potential model for C_{60} discussed above suggests the need not only for explicit representation of interaction sites on the short electron-rich bonds, but also electrostatic interactions. This completely empirical intermolecular potential is able to reproduce most experimental quantities rather well. The discrepancies that remain indicate a need for increased anisotropy of the molecules; a deficiency that could easily be corrected by further refining the parameters. Unfortunately, at the present time, an *ab initio* approach to solid C_{60} is difficult because of the large number (240) of carbon atoms in the $Pa\bar{3}$ unit cell (Feuston *et al.* 1991).

3. An alternative potential model for C_{60}

The structure of the orientationally ordered low-temperature phase of solid C_{60}, as discussed above, cannot be explained solely in terms of Lennard–Jones interactions between carbon atoms (Cheng & Klein 1992*a*, *c*). Recently, Lu *et al.* (1992) proposed an alternative extension of the atom–atom potential, in which positive and negative charge sites were positioned at the centres of the long and short carbon–carbon bonds respectively. In mean field theory, this version of the bond charge model exhibits a phase transition from a rotator phase to the experimentally observed ordered $Pa\bar{3}$ structure at about the correct temperature. Thus, the electrostatic contribution from bond charges alone proved sufficient to stabilize the $Pa\bar{3}$ structure.

We have examined the properties of the potential model proposed by Lu *et al.* (1992), using constant-pressure molecular dynamics (Nosé & Klein 1983). Figure 1 compares the cubic lattice parameters predicted for the models of Sprik *et al.* (1992) and Lu *et al.* (1992). The rotational ordering transition in the latter model occurs a little above the experimentally observed temperature, but is accompanied by only a marginal volume contraction. By contrast, the discontinuity calculated for the potential of Sprik *et al.* (1992) is much larger and in good agreement with experiment (Heiney *et al.* 1992), although the transition temperature is a little too low. The strikingly different behaviour exhibited by the two models can be

rationalized as follows: molecules in the ordered phase of the Sprik *et al.* potential fit together in a lock and key fashion and the unit cell volume is therefore reduced with respect to the rotator phase. This mechanism is far less pronounced for the potential of Lu *et al.* (1992) where the ordering is driven by electrostatic coupling. Apparently, a repulsive contribution arising from the electron density on the short bonds cannot be ignored.

4. Ground state at phase transition of solid C_{70}

As mentioned above, attempts to explain the stability of the $Pa\bar{3}$ ground state of C_{60} by means of simple atom–atom type interactions between C atoms were unsuccessful (Cheng & Klein 1992*a–c*). Extension of the model to include electrostatic interactions involving additional interaction sites on C–C bonds seemed to be required (Sprik *et al.* 1992; Lu *et al.* 1992). We propose herein a generalization of the Sprik *et al.* interaction model for C_{60} to the case of C_{70}. The potential is then used in an exploration of the solid-phase diagram, using constant pressure MD simulation, with no experimental input, other than the assumption of a FCC rotator phase at high temperatures (Vaughan *et al.* 1992).

The initial generalization of the C_{60} potential to C_{70} assumes that all C atoms can still be treated as a single type, with the C_{60} value for σ_C and q_C, even though in C_{70} these sites are no longer strictly equivalent (Fowler *et al.* 1991). Conceptually, the C_{70} molecule can be partitioned in two C_{60}-like 'polar caps', consisting of 20 atoms each, plus an 'equatorial' region of 30 atoms. The polar caps consist of a top pentagon and five hexagons, each sharing a long bond with the top pentagon. The 20 short bonds of these C_{60}-like caps are assigned D sites with the same σ_{DD} as in the C_{60} model and $q = -2q_C$. Of the bonds in the equatorial region, 30 have a length slightly larger than the short D bonds. These intermediate (I) bonds are grouped in five isolated hexagons. The remaining bonds have lengths more similar to the long bonds in C_{60}. On the basis of a length criterion and considerations of charge neutrality, we ignore the longer bonds and only include sites on I bonds with a σ_{II} ($= 3.5$ Å) chosen intermediate between the values for C and D sites and a charge $q_I = \frac{1}{2}q_D$. The radii for interactions between dissimilar pairs are determined by the arithmetic mean mixing rule. The value $\epsilon = 15$ K was used for all Lennard–Jones terms. The geometry of the rigid molecular C_{70} frame was taken from Andreoni *et al.* (1992).

According to experiment (Vaughan *et al.* 1992), in the high-temperature rotator phase I the FCC centre-of-mass structure is favoured over hexagonal close packed (HCP). The free energy difference between FCC and HCP is likely to be very small (Guo *et al.* 1991; Cheng & Klein 1992*c*). The simulation was initialized by setting up an orientationally disordered high-temperature state in a cubic MD box, which consisted of $4 \times 4 \times 4$ FCC 4-molecule unit cells with basis vectors $\boldsymbol{a}_{FCC}$, $\boldsymbol{b}_{FCC}$ and $\boldsymbol{c}_{FCC}$. The system size of 256 molecules with $\boldsymbol{L}_a = 4\boldsymbol{a}_{FCC}$ and $\boldsymbol{L}_c = 4\boldsymbol{c}_{FCC}$ was found to be necessary to minimize boundary effects. The simulation system was slowly cooled by applying the constant temperature-constant pressure MD technique (Sprik *et al.* 1992). Energies and forces were determined from a summation over all interaction sites on the 12 nearest and 6 next nearest neighbour molecules. The temperature was decreased in steps of 20 K (occasionally 10 K) after waiting at each state point 40–80 ps. The simulation, which effectively contains more than 30 000 atoms, was executed on a cluster of IBM RS/6000 workstations operating in parallel under the Parallel Virtual Machine (PVM) communication software (public domain) package (G. A. Geist & V. S. Sunderam). With cooling rates mentioned above, the total run time to follow

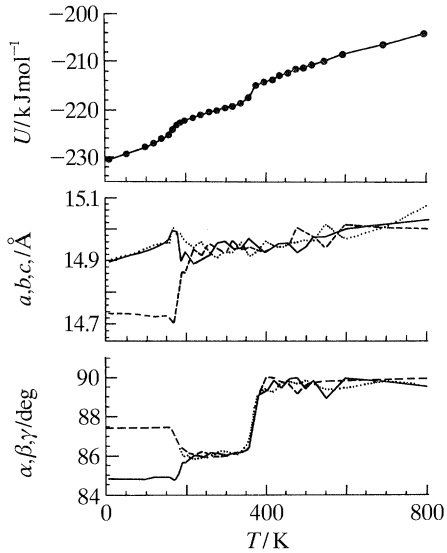

Figure 3. Calculated temperature dependence of selected properties of solid C_{70}. (*a*) The intermolecular potential energy, U; (*b*) MD box lengths plotted as cell vectors $\boldsymbol{a}_{\mathrm{FCC}} = \frac{1}{4}\boldsymbol{L}_{\mathrm{a}}$, $\boldsymbol{b}_{\mathrm{FCC}} = \frac{1}{4}\boldsymbol{L}_{\mathrm{b}}$, $\boldsymbol{c}_{\mathrm{FCC}} = \frac{1}{4}\boldsymbol{L}_{\mathrm{c}}$, and (*c*) angles between cell vectors.

the C_{70} system through two orientational ordering transitions was about three months.

The MD results, shown in figure 3, revealed two phase transitions. The first transition, $T_{\mathrm{I–II}}$, occurred around 380 K, and the second, $T_{\mathrm{II–III}}$, around 200 K. From the temperature dependence of the total interaction energy, U, we estimate the heats of transition as $\Delta H_{\mathrm{I–II}} = 2.8 \pm 0.3$ kJ mol^{-1} and $\Delta H_{\mathrm{II–III}} = 2.5 \pm 0.3$ kJ mol^{-1}. Vaughan *et al.* (1992) observed the I–II transition around 340 K, with $\Delta H_{\mathrm{I–II}} = 2.9 \pm 0.4$ kJ mol^{-1}, and the II–III transition around 280 K, with $\Delta H_{\mathrm{II–III}} = 2.3 \pm 0.4$ kJ mol^{-1}. These results agree surprisingly well with our calculations, the largest discrepancy being the value of $T_{\mathrm{II–III}}$. Vaughan *et al.* quote the FCC lattice constant in phase I at 325 K, just above the I–II phase transition, as $a = 14.96$ Å. At the corresponding point, we find a very similar value (see figure 3).

In constant-pressure molecular dynamics, any breaking of the point group symmetry can be monitored from the shape changes of the MD box (Parrinello & Rahman 1980). Figure 3 also shows the variation in lengths of the cell vectors $\boldsymbol{a}_{\mathrm{FCC}}$, $\boldsymbol{b}_{\mathrm{FCC}}$, $\boldsymbol{c}_{\mathrm{FCC}}$ and angles between them, α, β, γ, as a function of temperature. The I–II transition is accompanied by *ca.* 4° trigonal distortion, with virtually no change in the cell lengths. The corresponding transformation can be viewed as an elongation of a body diagonal of the cubic rotator phase I, which then becomes the trigonal phase II three-fold axis. We will refer to this particular [111] vector as $\boldsymbol{c}_{\mathrm{trg}}$. At the II–III transition, the trigonal symmetry is lost, but two of the angles and two of the lengths remain equal (see figure 3). The transformation compatible with this geometry is a shearing of the phase II rhombohedral MD box along a [110] vector c_{bct} intersecting with c_{trg}. If α_{bct} is the [001] vector coplanar with the pair ($\boldsymbol{c}_{\mathrm{trg}}$, $\boldsymbol{c}_{\mathrm{bct}}$) and $\boldsymbol{b}_{\mathrm{bct}}$, the [1$\bar{1}$0] vector perpendicular to this plane, then a $\boldsymbol{c}_{\mathrm{bct}}$ shear preserves the rectangular shape of the ($\boldsymbol{a}_{\mathrm{bct}}$, $\boldsymbol{b}_{\mathrm{bct}}$) plane. Thus, the predicted molecular centre-of-mass symmetry of phase III is monoclinic. Configurations taken from the three phases obtained in the MD calculations are shown in figure 4.

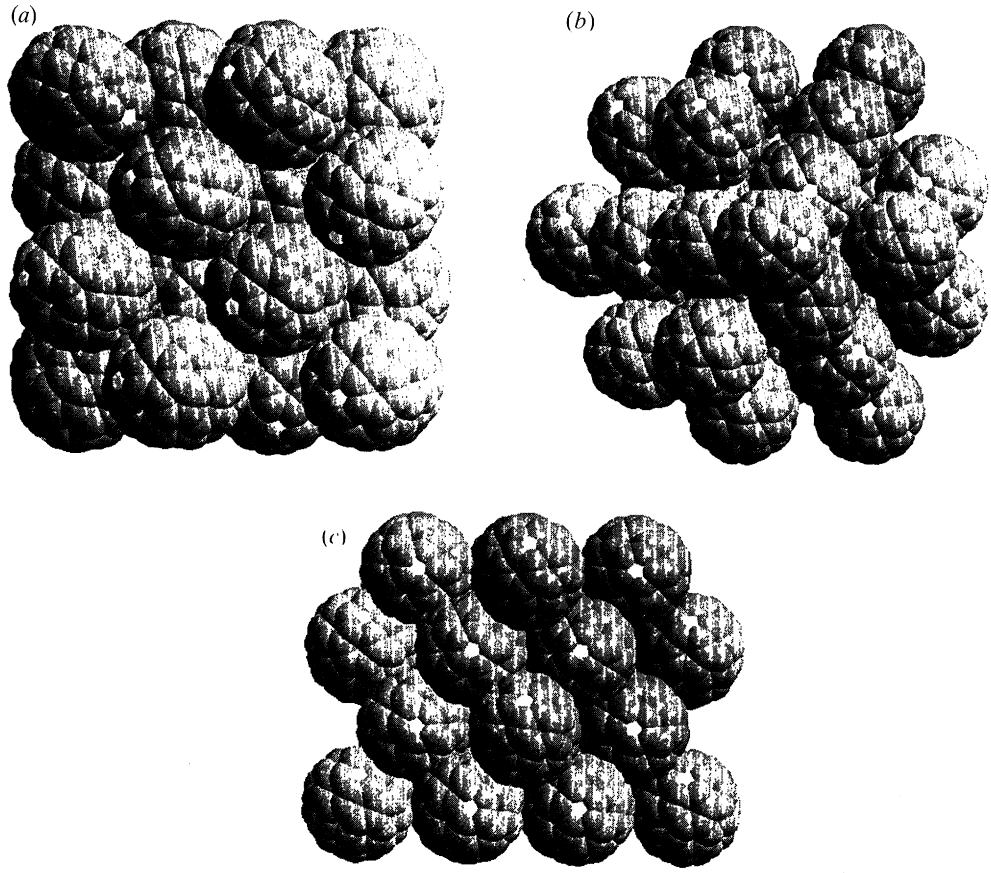

Figure 4. Instantaneous configurations taken from molecular dynamics simulations of the fullerene C_{70}. (*a*) The high-temperature ($T = 400$ K) rotator phase viewed from the $\langle 100 \rangle$ direction. (*b*) The intermediate phase viewed from the $\langle 111 \rangle$ direction. (*c*) The predicted low-temperature ($T = 10$ K) ordered phase viewed from the $\langle 110 \rangle$ direction.

With the relevant lattice directions identified, the nature of the orientational ordering can be analysed. To do so, Euler angle distributions $P(\theta), P(\phi)$ and $P(\psi)$ in the various phases have been calculated. Here, θ specifies the tilt orientation of the five-fold axis, with respect to $\boldsymbol{c}_{\mathrm{trg}}$. The azimuthal precession angle ϕ is measured with respect to the projection of $\boldsymbol{b}_{\mathrm{bct}}$ on the plane perpendicular to $\boldsymbol{c}_{\mathrm{trg}}$. The body rotation (spin) angle ψ is defined with respect to a two-fold axis of the C_{70} molecule. $P(\theta)$ is not completely isotropic in phase I, but is peaked in the six equivalent $\langle 110 \rangle$ directions. In the reference frame used here, the [110] vectors are divided into two groups, three are in the $\boldsymbol{c}_{\mathrm{trg}}$ [111] plane ($\theta = 90°$) and the other three have an inclination of $\theta = 35.3°$, with respect to $\boldsymbol{c}_{\mathrm{trg}}$. There is a somewhat surprising tendency for five-fold axis to point in $\langle 110 \rangle$ directions rather than $\langle 111 \rangle$, as is found with an atom–atom potential model (Cheng & Klein 1992*c*). However, despite the tilt, the long axes are still aligned, on average, along the trigonal axis $\boldsymbol{c}_{\mathrm{trg}}$. In phase II, $P(\phi)$ exhibits the same 120° modulation as in phase I, confirming that tilting towards $\langle 110 \rangle$ is preferred.

In phase III, the precessional disorder in $P(\phi)$ is removed and the competition between $\langle 111 \rangle$ and $\langle 110 \rangle$ alignment is resolved by half of the molecules orienting

along the [111] vector $\boldsymbol{c}_{\mathrm{bct}}$ ($\theta \approx 33°$, subsystem B). Simultaneously, the body axis rotation stops, at least on the MD timescale. $P(\psi)$, which was completely random in phases I and II, now splits into four peaks, each consisting of an A and B component. The AB fine structure does not show up as clear doublets because of orientational defects frozen in during the cooling process. Such an orientational glassy ground state may actually arise in the real crystal, even though it is non-cubic (Lewis & Klein 1987). However, the low-temperature structure we obtained in our simulation was sufficiently annealed to enable us to deduce an idealized phase III structure, which could then be further optimized by a steepest descent procedure.

The resulting ground state unit cell can be viewed as a monoclinic distortion of the phase I *bct* cell repeated in two of three directions, giving a unit cell containing 8 molecules and dimensions $a = 29.46$ Å, $b = 10.04$ Å, $c = 22.02$ Å, with angles $\angle\, ab = 90°$, $\angle\, bc = 90°$ and $\angle\, ac = 86.5°$. The orientations are arranged in layers AA′BB′ stacked along $\boldsymbol{c}$. The long axes of the A and A′ molecules are oriented almost perfectly in the $\boldsymbol{a}+2\boldsymbol{c}$ direction. The B and B′ molecules point along $\boldsymbol{c}$. In a given layer, the molecules are organized in rows with identical orientations parallel to $\boldsymbol{b}$ and alternating in the $\boldsymbol{a}$ direction.

5. Conclusions

The constant-pressure molecular dynamics technique implemented on a cluster of IBM RS/6000 workstations, operating in parallel, has enabled us to characterize possible structures of solid C_{70} unbiased by *a priori* assumptions about the orientational order.

In accordance with experimental observation and some earlier simulation results (Cheng & Klein 1992*c*) on an atom–atom model, we find orientational ordering in solid C_{70} to occur in two stages. Cooling the high-temperature phase I, produces an intermediate phase II, in which the long (five-fold) axes are oriented with a small but distinct tilt (*ca.* 18°) with respect to a unique ⟨111⟩ direction. Molecular rotations about the five-fold body axis still occur. A second type of motion, which consists of 120° precessional jumps, restores the ordering ⟨111⟩ direction as a threefold symmetry axis. Then, in the fully ordered phase III, half of the molecules align almost exactly along this direction ⟨111⟩ and the other half along ⟨110⟩. The competition between the ⟨111⟩ and ⟨110⟩ orientations is a consequence of a particular feature of the potential, namely repulsive interactions between C–C bonds. When the interactions are described in the simple atom–atom approximation, this curious effect is not observed and all molecules point in a common ⟨111⟩ direction in both phases II and III.

The models described herein can be extended to treat the alkali metal (M) doped fullerenes M_xC_{60} (Cheng & Klein 1991*a*,*b*) and compounds, such as $C_{60}O$ (Cheng & Klein 1992*b*), but space limitations preclude any discussion of these systems. The interested reader is referred to the original articles for details.

We are grateful to Roger Larsson for installing the PVM communications software and assisting us with the parallelization of the molecular dynamics code, and François Gygi, Paul Heiney, J. E. Fischer for useful suggestions. Both A.C. and M.L.K. thank the U.S. National Science Foundation for support.

References

Allen, M. P. & Tildesley, D. J. 1987 *Computer simulation of liquids*. Oxford: Clarendon Press.

Andreoni, W., Gygi, F. & Parrinello, M. 1992 Structural and electronic properties of C_{70}. *Chem. Phys. Lett.* **189**, 241–244.

Cheng, A. & Klein, M. L. 1991*a* Molecular dynamics simulations of solid Buckminsterfullerenes. *J. phys. Chem.* **95**, 6750–6751.

Cheng, A. & Klein, M. L. 1991*b* Molecular dynamics investigation of alkali-metal-doped fullerites. *J. phys. Chem.* **95**, 9622–9625.

Cheng, A. & Klein, M. L. 1992*a* Molecular dynamics investigation of orientational freezing in solid C_{60}. *Phys. Rev.* B**45**, 1889–1895.

Cheng, A. & Klein, M. L. 1992*b* $C_{60}O$: A molecular dynamics study of rotation in the solid phase. *J. chem. Soc. Faraday Trans.* **88**, 1949–1951.

Cheng, A. & Klein, M. L. 1992*c* Solid C_{70}: A molecular dynamics study of structure and orientational ordering. *Phys. Rev.* B. **46**, 4958–4965

Copley, J. D. R., Neumann, D. A. & Cappalletti, R. L. 1992 Structure and low energy dynamics of Solid C_{60}. *Physica* B. (In the press.)

David, W. I. F., Ibberson, R. M. & Mathewman, J. C. 1991 Crystal structure and bonding of ordered C_{60}. *Nature, Lond.* **353**, 147–149.

David, W. I. F., Ibberson, R. M., Dennis, T. J. S., Hare, J. P. & Prassides, K. 1992 Structural phase transitions in the fullerene C_{60}. *Eur. Phys. Lett.* **18**, 219–225.

Dworkin, A., Szwarc, H. & Leach, S. 1991 Mise en évidence thermodynamique d'une transition de phase dans le fulleréne C_{60} cristallin. *C.r. Acad. Sci., Paris* II **312**, 979–982.

Feuston, B. P., Andreoni, W., Parrinello, M. & Clementi, E. 1991 Electronic and vibrational properties of C_{60} at finite temperature from *ab initio* molecular dynamics. *Phys. Rev.* B **44**, 4056–4059.

Fowler, P. W., Lazzeretti, P. & Zanasi, R. 1990 Electric and magnetic properties of the aromatic sixty-carbon cage. *Chem. Phys. Lett.* **165**, 79–86.

Fowler, P. W., Lazzeretti, P., Malagoli, M. & Zanasi, R. 1991 Magnetic properties of C_{60} and C_{70}. *Chem. Phys. Lett.* **179**, 174–180.

Guo, Y., Karasawa, N. & Goddard III, W. A. 1991 Prediction of fullerene packing in C_{60} and C_{70} crystals. *Nature, Lond.* **351**, 464–467.

Heiney, P. A. *et al.* 1991 Orientational phase transition in solid C_{60}. *Phys. Rev. Lett.* **66**, 2911–1468.

Heiney, P. A. *et al.* 1992 Discontinuous volume change at the orientational-ordering transition in solid C_{60}. *Phys. Rev.* B**45**, 4544–4547.

Johnson, R. D., Meijer, G., Salem, J. R. & Bethune, D. S. 1991 Two-dimensional nuclear resonance study of the structure of the fullerene C_{70}. *J. Am. chem. Soc.* **113**, 3619–3621.

Johnson, R. D., Yannoni, C. S. & Dorn, H. C. 1992 C_{60} rotation in the solid state: Dynamics of a faceted spherical top. *Science, Wash.* **255**, 1235–1238.

Kriza, G. *et al.* 1991 Pressure dependence of the structural phase transition in C_{60}. *J. Phys. I* **1**, 1361–1364.

Lewis, L. J. & Klein, M. L. 1987 Is the ground state of (KCl)(KCN) a non-cubic orientational glass? *Phys. Rev. Lett.* **59**, 1837–1840.

Lu, J. P., Li, X.-P. & Martin, R. M. 1992 Ground state and phase transitions in solid C_{60}. *Phys. Rev. Lett.* **68**, 1551–1554.

Michel, K. H., Copley, J. D. R. & Neumann, D. A. 1992 Molecular theory of orientational disorder and the orientational phase transition in solid C_{60}. *Phys. Rev. Lett.* **68**, 2929–2932.

Neumann, D. A. *et al.* 1991 Coherent quasielastic neutron scattering study of rotational dynamics of C_{60} in the orientationally disordered phase. *Phys. Rev. Lett.* **67**, 3808–3811.

Nosé, S. & Klein, M. L. 1983 Constant pressure molecular dynamics for molecular systems. *Molec. Phys.* **50**, 1055–1076.

Pan, C., Sampson, M. P., Chai, Y., Hauge, R. H. & Margrave, J. L. 1991 Heats of sublimation from a polycrystalline mixture of C_{60} and C_{70}. *J. phys. Chem.* **95**, 2944–2946.

PHILOSOPHICAL TRANSACTIONS OF THE ROYAL SOCIETY A MATHEMATICAL, PHYSICAL & ENGINEERING SCIENCES

Parrinello, M. & Rahman, A. 1980 A new constant pressure molecular dynamics. *Phys. Rev. Lett.* **45**, 1196–1199.

Raich, J. & Mills, R. L. 1971 α–γ Transition in solid nitrogen and carbon monoxide at high pressure. *J. chem. Phys.* **55**, 1811–1187.

Sachidanandum, R. & Harris, A. B. 1991 Comment on: Orientational phase transition in solid C_{60}. *Phys. Rev. Lett.* **67**, 1467.

Shi, X. D., Kortan, A. R., Williams, J. M., Kini, A. M., Savall, B. M. & Chaiken, P. M. 1992 Sound velocity and attenuation in single-crystal C_{60}. *Phys. Rev. Lett.* **68**, 827–830.

Sprik, M., Cheng, A. & Klein, M. L. 1992 Modelling the orientational ordering transition in solid C_{60}. *J. phys. Chem.* **96**, 2027–2029.

Taylor, R., Hare, J. P., Abdul-Sada, A. K. & Kroto, H. W. 1990 Isolation, separation and characterization of the fullerenes C_{60} and C_{70}: The third form of carbon. *J. chem. Soc. chem. Commun.* 1423–1425.

Tycko, R., Dabbagh, R. M., Flemming, R. M., Haddon, R. C., Makhija, A. V. & Zahurak, S. M. 1991*a* Molecular dynamics and phase transition in solid C_{60}. *Phys. Rev. Lett.* **67**, 1886–1889.

Tycko, R. *et al.* 1991*b* Solid-state magnetic resonance spectroscopy of fullerenes. *J. phys. Chem.* **95**, 518–520.

van Loosdrecht, P. H. M., van Bentum, P. J. M. & Meijer, G. 1992 Rotational ordering transition in single-crystal C_{60} studied by Raman spectroscopy. *Phys. Rev. Lett.* **68**, 1176–1179.

Vaughan, G. B. M. *et al.* 1992 Orientational disorder in solvent-free solid C_{70}. *Science, Wash.* **254**, 1350–1353.

Yannoni, C. S., Johnson, R. D., Meijer, G., Bethune, D. S. & Salem, J. R. 1991 *J. phys. Chem.* **95**, 9–10.

Discussion

M. Lal (*Unilever Research, Port Sunlight Laboratory, U.K.*): The maximum time covered in your MD simulations is 200 ps. How did you establish that the water molecules at the monolayer of the hydrocarbon chain molecules have attained the equilibrium state in the droplet form in coexistence with vapour? If the initial water layer was several molecules thick, would you then expect that the equilibrium state would be the one in which a residual monolayer of water molecules exists in equilibrium with the droplet?

M. L. Klein: The equilibrium state was checked in the usual fashion. For example, we monitor the height of the droplet's centre of mass as a function of time, the radial density profile, energy, etc. We are confident that our results (J. Hautman & M. L. Klein, *Phys. Rev. Lett.* **67**, 1763–1766 (1991)) are indeed correct.

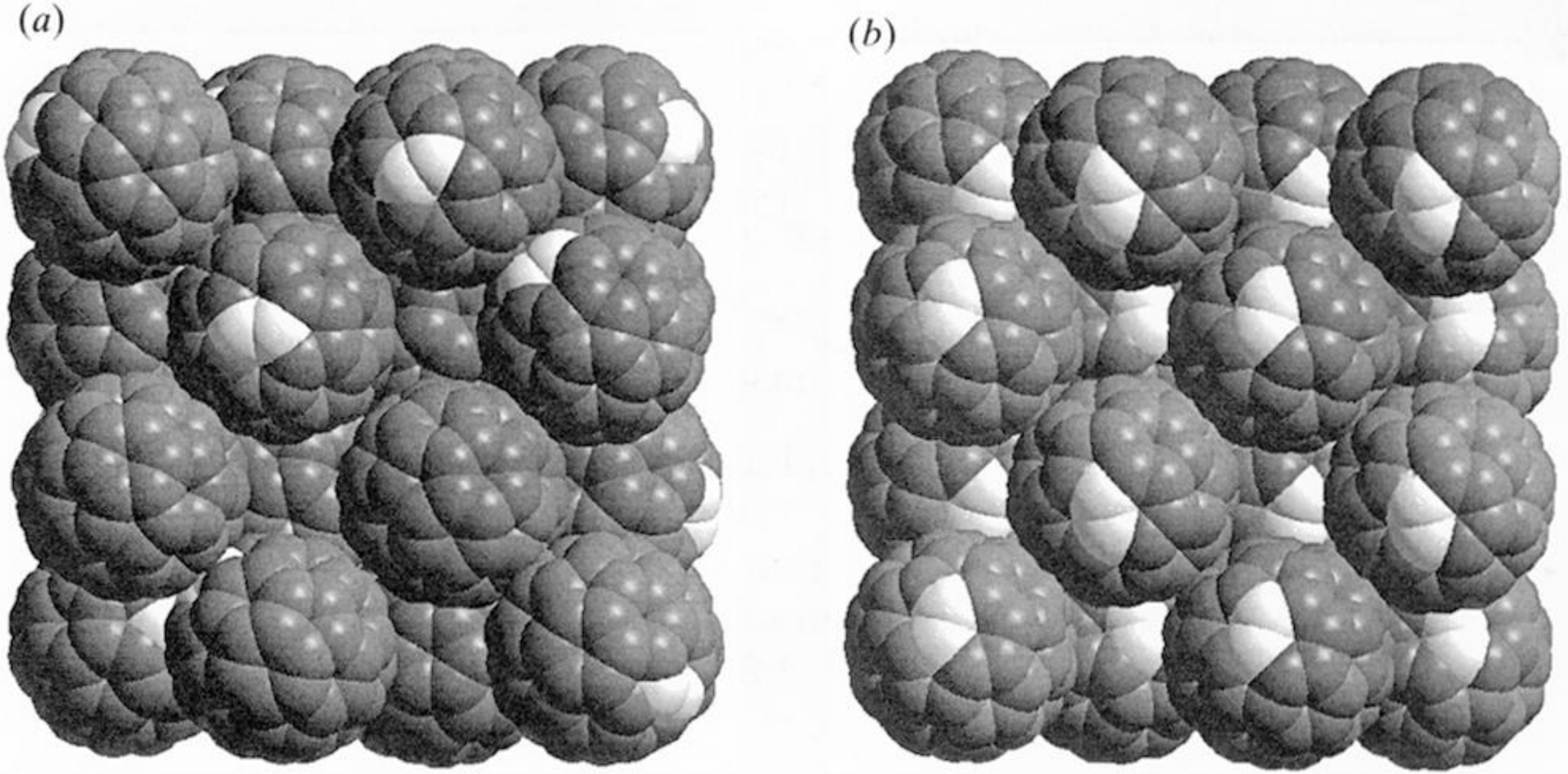

Figure 2. Instantaneous configurations taken from molecular dynamics simulations of the ullerene C_{60}. (*a*) The room-temperature rotator phase. (*b*) The low-temperature ordered phase.

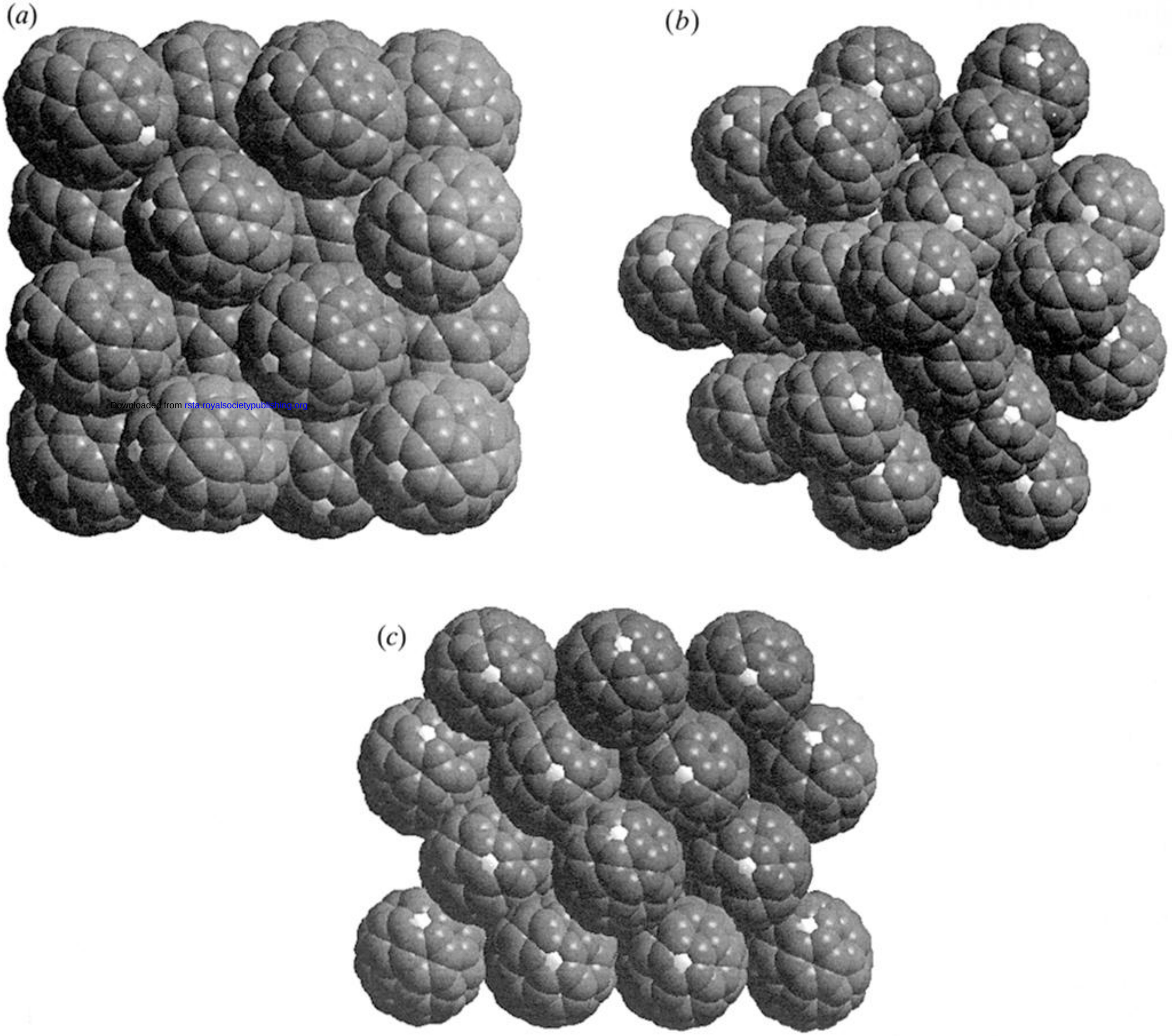

Figure 4. Instantaneous configurations taken from molecular dynamics simulations of the fullerene C_{70}. (*a*) The high-temperature ($T = 400$ K) rotator phase viewed from the $\langle 100 \rangle$ direction. (*b*) The intermediate phase viewed from the $\langle 111 \rangle$ direction. (*c*) The predicted low-temperature ($T = 10$ K) ordered phase viewed from the $\langle 110 \rangle$ direction.